CHEMICAL KINETIC AND DIFFUSIONAL LIMITATIONS ON BICARBONATE REABSORPTION BY THE PROXIMAL TUBULE

KENNETH W. WANG AND WILLIAM M. DEEN, *Department of Chemical Engineering, Massachusetts Institute of Technology, Cambridge, Massachusetts 02139 U.S.A.*

ABSTRACT It is widely accepted that bicarbonate reabsorption in the proximal tubule is mediated by H^+ secretion, but several aspects of this process have remained controversial. To examine some of these issues, we have developed a model that allows for spatial variations in the concentrations of CO_2, HCO_3^-, and H_2CO_3 within the tubule lumen and cell cytoplasm, passive transport of these substances across cell membranes, carbonic anhydrase-catalyzed interconversion of HCO_3^- and CO_2 within the cell and at the luminal membrane surface, and the corresponding uncatalyzed reactions in lumen and cell. Most of the required kinetic and transport parameters were estimated from physicochemical data in the literature, whereas intracellular pH and HCO_3^- permeability at the basal cell membrane, found to be the most significant parameters under normal conditions, were adjusted to yield reabsorption rates of "total CO_2" (tCO_2, the sum of CO_2, HCO_3^- and H_2CO_3) comparable to measured values in the rat. Our results suggest that for normal carbonic anhydrase activity, almost all tCO_2 leaves the lumen as CO_2, yet the transepithelial difference in CO_2 partial pressure does not exceed ~2 mm Hg. Electrochemical potential gradients favor substantial passive backleak of HCO_3^- from cell to lumen. Gradients in CO_2 partial pressure remain small during simulated inhibition of carbonic anhydrase, with ~70% of tCO_2 leaving the lumen as H_2CO_3 in this case, and the remainder as CO_2. Predicted tCO_2 reabsorption rates for carbonic anhydrase inhibition are ~25% of normal, in good agreement with recent measurements in the rat, indicating that the concept of "carbonic acid recycling" is viable.

INTRODUCTION

Renal regulation of plasma bicarbonate concentration plays a critical role in the control of blood pH. Under normal circumstances it is required that most or all of the bicarbonate appearing in glomerular filtrate be returned to the circulation by reabsorption across the renal tubule and subsequent uptake by the surrounding peritubular capillaries; the bulk of this reabsorption (typically 80–90%) is accomplished by the proximal convoluted tubule. Accordingly, the mechanism of bicarbonate reabsorption in this tubule segment has received extensive study, as discussed in several recent reviews (1–5).

A generally accepted view of this process is depicted in Fig. 1. The primary event is believed to be active secretion of H^+ from epithelial cell to tubule lumen, which titrates luminal HCO_3^- to form H_2CO_3 and CO_2. These substances (primarily CO_2) are thought to diffuse

---

Mr. Wang's present address is Union Carbide Corporation, Bound Brook, N. J. 08805

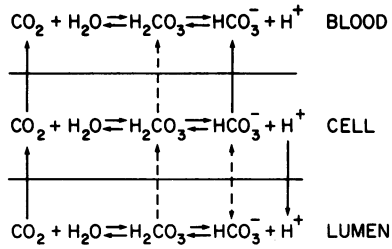

FIGURE 1 Principal features of the bicarbonate reabsorption process in the proximal tubule. Transport steps generally accepted as playing an important role are shown by solid arrows; those of more questionable significance are shown by dashed arrows.

back into the cell, supplying substrates for the continued intracellular generation of HCO_3^- and H^+. The HCO_3^- formed by the intracellular reaction diffuses preferentially into the peritubular interstitium and blood, thereby accomplishing net reabsorption of HCO_3^-. As shown in Fig. 1, some of the reabsorbed HCO_3^- may be transported across the cell in the form of CO_2 (or H_2CO_3), which reequilibrates with HCO_3^- in the blood. The overall process is most often characterized in terms of the reabsorption rate of "total CO_2," abbreviated tCO_2, which refers to the sum of HCO_3^-, CO_2, and H_2CO_3.

Several aspects of the scheme shown in Fig. 1 remain controversial. The enzyme carbonic anhydrase is present in the renal cortex and is known to catalyze the interconversion of HCO_3^- and CO_2. It has been hypothesized that membrane-bound carbonic anhydrase normally prevents the accumulation of significant amounts of H_2CO_3 in the lumen by facilitating its conversion to CO_2, while catalyzing the reverse reaction (CO_2 hydration) in the cell (1). During administration of carbonic anhydrase inhibitors such as acetazolamide, bicarbonate reabsorption may continue at as much as 20–50% of the normal rate (6–8), and it has been suggested (1) that this is made possible by H_2CO_3 diffusion from lumen to cell ("carbonic acid recycling"). Other explanations have been offered, including direct reabsorption of HCO_3^- (4). The magnitude of the transepithelial difference in CO_2 concentration (tubule lumen minus blood), relating to the question of whether the epithelium is a significant diffusion barrier for CO_2, has been another source of controversy (2,9–11).

Many of the physiological questions raised are of a quantitative nature, involving rates of chemical reaction and mass transfer, and may be answered or at least clarified using a suitable theoretical model. A compartmental model has been employed by Cassola et al. (12) in the interpretation of data obtained using the stationary microperfusion technique, but it considers only "total hydrogen ion content" in each compartment and is not sufficiently detailed to examine the influence of the various reaction and diffusion steps. In the model presented here we have endeavored to include the principal reactions and mass transfer processes involving tCO_2 within the tubule lumen, cell cytoplasm, and cell membranes. Although this formulation undoubtedly is still a considerable oversimplification, a sizeable number of anatomic, kinetic, and transport parameters is required. Reasonable estimates of most of these can be obtained from the literature, enabling us to focus on a few variables that appear to be critical in the reabsorption of bicarbonate.

LIST OF SYMBOLS

a_I, a_K Integration constants in Eq. 21.
b_{1i}, b_{2i} Functions of η in Eq. 35.
C_i Concentration of solute i (molar units).
$\bar{C}_i$ Bulk concentration of solute i in lumen, Eq. 41.
D_i Diffusivity of solute i.
f Fraction of reabsorbed water crossing cell.
F Faraday's constant.
J_{tCO_2} Reabsorption rate of total CO_2 per unit length of tubule.
k_n, k_{-n} Forward and reverse rate constants, respectively, for reaction n. Rate constants for catalyzed heterogeneous reaction at brush border membrane are k_{4s} and k_{-4s}.
k_t Overall intracellular reaction rate constant, $k_1 + k_4$.
K_n Equilibrium constant for reaction n, k_n/k_{-n}.
L Tubule length.
m Constant defined by Eq. 22 or Eq. 44.
N_i Radial flux of solute i (per unit area).
N_{im} Flux of solute i across cell membrane (per unit area).
P_{CO_2} Partial pressure of CO_2.
P_i Membrane permeability to solute i.
r Radial coordinate, $r = r_1$ at brush border and $r = r_2$ at basal membrane (Fig. 2).
R Gas constant.
S_i Volumetric rate of formation of species i in lumen.
$S_{ic}^{(j)}$ Volumetric rate of formation of species i by reaction j in cell.
T Absolute temperature.
$T_1 - T_5$ Constants defined by Eqs. 11, 12, 16, 20, and 23 or 45, respectively.
tCO_2 "Total CO_2," the sum of CO_2, HCO_3^-, and H_2CO_3.
v_0 Mean axial fluid velocity in lumen at $z = 0$.
v_{rl} Radial fluid velocity in lumen at $r = r_1$.
v_{rc} Radial fluid velocity in cell, function of r.
v_z Axial fluid velocity in lumen, function of r and z.
z Axial coordinate (Fig. 2).

Greek Letters

η Dimensionless axial coordinate, z/r_1.
ξ Dimensionless radial coordinate, r/r_1.
$\phi_i^{(j)}$ Rate of formation of species i per unit surface area by heterogeneous reaction j.
$\Delta\psi_1, \Delta\psi_2$ Dimensionless electrical potential differences across cell membranes, relative to RT/F. See Eq. 27.

Subscripts

b Quantity evaluated in peritubular plasma or interstitial fluid.
c Quantity evaluated within cell cytoplasm.
i Chemical species identification, 1 = CO_2, 2 = HCO_3^-, 3 = H_2CO_3, and 4 = H^+.

DESCRIPTION OF MODEL

General Considerations

A schematic diagram of the mammalian proximal tubule is shown in Fig. 2. The epithelium consists of a single layer of cuboidal cells ~10 μm thick, and will be represented here as a

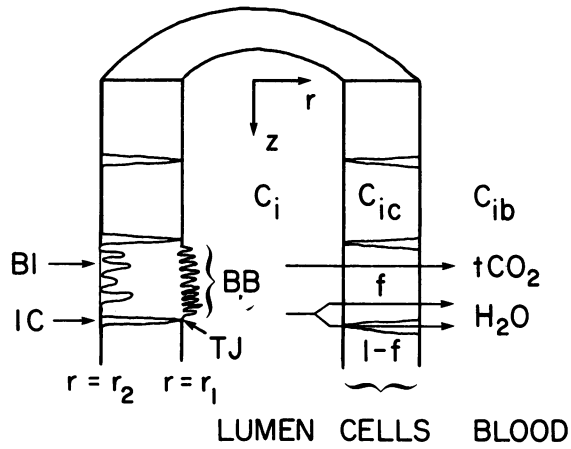

FIGURE 2 Schematic representation of mammalian proximal tubule. Anatomical features of the epithelium are indicated as follows: BI, basal infoldings; IC, intercellular channels; BB, brush border; TJ, tight junction. See text for additional explanation.

circular cylinder of inner radius r_1 (~15 μm for the rat) and outer radius r_2 (~25 μm). Membrane thicknesses are of course negligible compared with r_1 or r_2. Radial and axial coordinates are defined as shown, with $z = 0$ representing the junction between the proximal tubule and Bowman's capsule, or in the case of tubule perfusion experiments, the site of the perfusion pipet. Concentrations of solute i in the tubule lumen (C_i) and cell cytoplasm (C_{ic}) are functions of r and z, while concentrations in peritubular interstitial fluid (C_{ib}) are taken to be independent of position. The interstitial concentrations are assumed to be similar to those in peritubular capillary plasma since the capillary endothelium is expected to offer little resistance to the transport of carbon dioxide, bicarbonate, and related substances. Throughout this paper, the subscript i will be used to identify the chemical species as follows:

$$\begin{aligned} i = 1 &: CO_2 \\ 2 &: HCO_3^- \\ 3 &: H_2CO_3 \\ 4 &: H^+ \end{aligned}$$

Unless otherwise indicated, summations are understood to be over the index i, from 1 to 3 only.

In this part of the nephron an isotonic reabsorbate containing mostly sodium, bicarbonate, and chloride is transported across the epithelium. Fluid and solute transport may occur via transcellular or paracellular pathways (Fig. 2), the latter through "tight junctions" (TJ) and intercellular channels (IC). Although both routes may be significant for fluid reabsorption, it is assumed that only the transcellular pathway is important for movement of tCO_2. Some convective transport of bicarbonate may take place through the intercellular channels, but this will be opposed by a diffusive backleak of bicarbonate from interstitium to tubule lumen. The plasma membrane at the luminal side of the cells forms a brush border (BB) consisting of numerous microvilli, and the membrane at the basal or pertibular side of the cell also is not "flat," having a number of invaginations, basal infoldings (BI) (13). This fine structure will

not be considered, except that when solute permeabilities are estimated using data from other membranes (e.g., red cell or lipid bilayer), their values will be increased according to the ratio of true membrane area at either side of the cell to that of the idealized cylinder (14).

CHEMICAL REACTIONS Consideration will be limited to water, hydrogen, and hydroxyl ions, and the "CO_2-containing" species, CO_2, HCO_3^-, and H_2CO_3. Carbonate ($CO_3^=$) has been omitted from this list, since in the pH range of interest (<8), it accounts for <1% of tCO_2 (15), and is unlikely to be transported across cell membranes to any significant extent because of its charge. Although several studies have linked hydrogen secretion to sodium reabsorption (2), and exchange of chloride for bicarbonate may also play a role in the acidification process (1), the mechanisms of these effects remain poorly understood, and a model that takes explicit account of sodium and chloride transport does not at present appear feasible. Phosphate or other buffers present in the luminal fluid may also influence the process, but throughout much of the proximal tubule they are present in substantially smaller concentrations than bicarbonate and will also be neglected.

Several pathways exist for the interconversion of CO_2, HCO_3^-, and H_2CO_3 and these will be referred to as catalyzed or uncatalyzed, according to whether or not carbonic anhydrase is involved. The terms homogeneous and heterogeneous will denote reactions taking place throughout the volume of a compartment and those occurring at a membrane surface, respectively. The former will appear as source terms in the differential equations, and the latter in the boundary conditions.

Two mechanisms exist for the uncatalyzed reaction of CO_2 to HCO_3^-, as discussed by Kern (16):

$$H_2O + CO_2 \underset{k_{-1}}{\overset{k_1}{\rightleftharpoons}} H_2CO_3 \underset{k_{-2}}{\overset{k_2}{\rightleftharpoons}} H^+ + HCO_3^- \qquad \text{(reactions 1 and 2)}$$

$$OH^- + CO_2 \underset{k_{-3}}{\overset{k_3}{\rightleftharpoons}} HCO_3^- \qquad \text{(reaction 3)}$$

The second mechanism (reaction 3) may be quite significant at very alkaline pH, but at pH 7.6 and below (our range of interest) the product of k_3 and hydroxyl concentration is <10% of k_1 (16), and only the first mechanism will be considered. With regard to the catalyzed reaction, carbonic anhydrase is frequently depicted as affecting the hydration of CO_2 to H_2CO_3, but there is evidence that the substrates are actually OH^- and CO_2 (17). We will adopt this view, which is analogous to reaction 3 above, in which H_2CO_3 is not formed as an intermediate. When this reaction is added to that for the dissociation of water, the net reaction for the catalyzed case becomes:[1]

$$H_2O + CO_2 \underset{k_{-4}}{\overset{k_4}{\rightleftharpoons}} HCO_3^- + H^+ \quad \text{(C.A.)} \qquad \text{(reaction 4)}$$

[1]As discussed by Kernohan et al. (18), carbonic anhydrase is only slightly combined with substrate and product under physiological conditions, so that the hydration reactions are approximately first order with respect to CO_2 and HCO_3^- concentrations, respectively. The pseudo-first-order rate constants are denoted here by k_4 and k_{-4}.

It is assumed that the hydration of CO_2 in the cell cytoplasm involves only homogeneous reactions, with the catalyzed and uncatalyzed pathways proceeding in parallel. Since there is evidence that luminal fluid is in contact with carbonic anhydrase (1), a heterogeneous, catalyzed hydration of CO_2 is assumed to occur at the luminal surface of the brush-border membrane (at $r = r_1$). Homogeneous uncatalyzed reactions may also take place in the lumen (reactions 1 and 2). However, since the intrinsic rate of reaction 2 is very large, this reaction may be considered to be at equilibrium except in a very thin layer of fluid adjacent to the site of H^+ secretion at $r = r_1$. Using the analysis of Smith et al. (19), the thickness of this region is estimated to be only a few ångströms, so that reaction 2 in the lumen will be viewed as heterogeneous. Reaction 1 is considered to proceed at a slow but finite rate throughout the tubule lumen. Additional information on the reaction kinetics and equilibria are given below.

Intracellular Transport

Transport in the intracellular compartment is assumed to occur only in the radial direction. A key quantity is the intracellular pH, for which there does not appear to be any measurements in the proximal tubule. The high mobility of H^+ and the probable facilitation of H^+ transport by various intracellular buffers (20) suggest that large pH gradients probably do not exist within the cell, and that it is reasonable to assume that intracellular pH is independent of position. Possible variations in intracellular (as well as luminal) electrical potential will also be neglected, although measured transmembrane potential differences will be taken into account.

With these assumptions, species conservation equations for the intracellular region are required only for CO_2, HCO_3^- and H_2CO_3. The molar flux of species i in the radial direction within cell (N_{ic}) is given by:

$$N_{ic} = v_{rc} C_{ic} - D_{ic} \frac{\partial C_{ic}}{\partial r}, \tag{1}$$

where v_{rc} is the r-component of the intracellular fluid velocity, C_{ic} is the intracellular concentration of species i, and D_{ic} is the diffusion coefficient. Conservation of species i may be expressed as (21):

$$D_{ic} \frac{\partial^2 C_{ic}}{\partial r^2} + \frac{1}{r} (D_{ic} - v_{rc} r) \frac{\partial C_{ic}}{\partial r} = - \sum_j S_{ic}^{(j)}, \tag{2}$$

where $S_{ic}^{(j)}$ is the volumetric rate of formation of species i by reaction j. When Eq. 2 is applied to CO_2, an additional source term should in principle be added to the right side to account for metabolic production of CO_2. Although difficult to evaluate with precision, the metabolic contribution is estimated to be small and will be neglected.[2]

[2]A rough estimate of the rate of metabolic production of CO_2 can be obtained from the O_2 consumption rate for the whole kidney given by Cohen and Kamm (38), ~270 μmol O_2 (100 g)$^{-1}$ min^{-1}. Applying this figure to the proximal tubule and using a tubule outer radius of 25 μm, a specific gravity of 1.0 and a respiratory quotient of 1.3, one obtains a CO_2 production rate per unit tubule length of ~7 pmol mm^{-1} min^{-1}. This is much smaller than the normal tCO_2 reabsorption rate of ~150 pmol mm^{-1} min^{-1} (33). During acetazolamide infusion, sodium reabsorption by the proximal tubule is markedly reduced (6,33), and if the direct relationship between sodium reabsorption and O_2 consumption observed in other circumstances (38) is preserved, metabolic production of CO_2 should continue to be a small fraction of tCO_2 reabsorption.

TABLE I
REFERENCE VALUES FOR MODEL PARAMETERS

Diffusivities ($cm^2\ s^{-1}$)	
$D_1 = 1.72 \times 10^{-5}$	$D_{1c} = 7.6 \times 10^{-6}$
$D_2 = 1.17 \times 10^{-5}$	$D_{2c} = 4.0 \times 10^{-6}$
$D_3 = 1.17 \times 10^{-5}$	$D_{3c} = 4.0 \times 10^{-6}$
Permeabilities ($cm\ s^{-1}$)	
$P_1(r_1) = 5.4$	$P_1(r_2) = 3.0$
$P_2(r_1) = 2.0 \times 10^{-5}$	$P_2(r_2) = 7.0 \times 10^{-5}$
$P_3(r_1) = 3.6 \times 10^{-2}$	$P_3(r_2) = 2.0 \times 10^{-2}$
Reaction rate and equilibrium constants	
$K_1 = 2.94 \times 10^{-3}$	$k_1 = 0.15\ s^{-1}$
$K_2 = 2.7 \times 10^{-7}$ mol cm^{-3}	$k_{4s} = 1.0$ cm s^{-1}
$K_4 = 7.94 \times 10^{-10}$ mol cm^{-3}	
Solute concentrations	
$C_{1b} = 1.204 \times 10^{-6}$ mol cm^{-3}	$pH_b = 7.4$
$C_{2b} = 2.4 \times 10^{-5}$ mol cm^{-3}	$pH_c = 7.0$
$C_{3b} = 3.54 \times 10^{-9}$ mol cm^{-3}	
Other quantities	
$r_1 = 1.5 \times 10^{-3}$ cm	$\Delta\psi_1 = -2.51$
$r_2 = 2.5 \times 10^{-3}$ cm	$\Delta\psi_2 = +2.62$
$v_0 = 3.6 \times 10^{-2}$ cm s^{-1}	f = 0.5
$v_{rl} = 4.1 \times 10^{-5}$ cm s^{-1}	

Provided that intracellular fluid flow is only in the radial direction, it is easily shown that the product rv_{rc} is a constant. Further, it is assumed that v_{rc} can be related to the radial velocity in the lumen by

$$rv_{rc} = f r_1 v_{rl} \tag{3}$$

where v_{rl} is the radial component of the luminal fluid velocity evaluated at the membrane ($r = r_1$), and f is the fraction of reabsorbed fluid that passes across the cells, as distinguished from that moving through intracellular channels. Eq. 3 disregards the variations in radial velocities with z that may occur on the length scale of a single cell (10^{-3} cm), since tubule lengths are some two orders of magnitude larger than this. Substituting Eq. 3 into Eq. 2, and noting that $f r_1 v_{rl}$ is smaller than D_{ic} by about two orders of magnitude (Table 1), it is clear that convection has little effect on the intracellular concentration profiles and may be safely neglected. Introducing a dimensionless radial coordinate, $\xi = r/r_1$, the conservation equations for the three species may now be written:

$$-\frac{D_{1c}}{r_1^2}\nabla_\xi^2 C_{1c} = S_{1c}^{(1)} + S_{1c}^{(4)} \tag{4}$$

$$-\frac{D_{2c}}{r_1^2}\nabla_\xi^2 C_{2c} = S_{2c}^{(2)} + S_{2c}^{(4)} \tag{5}$$

$$-\frac{D_{3c}}{r_1^2}\nabla_\xi^2 C_{3c} = S_{3c}^{(1)} + S_{3c}^{(2)}, \tag{6}$$

where

$$\nabla_\xi^2 \equiv \frac{1}{\xi}\frac{\partial}{\partial \xi}\left(\xi \frac{\partial}{\partial \xi}\right), \xi \equiv r/r_1.$$

The reaction rates are given by

$$S_{1c}^{(4)} = k_{-4}C_{2c}C_{4c} - k_4 C_{1c} = -S_{2c}^{(4)} \tag{7}$$

$$S_{1c}^{(1)} = k_{-1}C_{3c} - k_1 C_{1c} = -S_{3c}^{(1)} \tag{8}$$

$$S_{2c}^{(2)} = k_2 C_{3c} - k_{-2}C_{2c}C_{4c} = -S_{3c}^{(2)}. \tag{9}$$

In solving for the concentration profiles it is convenient to deal with the sum of Eqs. 4–6, which yields a conservation equation for tCO_2 in which the reaction terms no longer appear. This may be integrated twice to give

$$\Sigma D_{ic}C_{ic} = T_1 \ln \xi + T_2 \tag{10}$$

$$T_1 = \Sigma D_{ic}[C_{ic}(r_2/r_1) - C_{ic}(1)]/\ln(r_2/r_1) \tag{11}$$

$$T_2 = \Sigma D_{ic}C_{ic}(1). \tag{12}$$

Additional steps in the solution depend on the reaction kinetics. For the normal (catalyzed) case, two of the three reactions (2 and 4) are extremely fast, and according to the method of Olander (22), may be assumed to be in local equilibrium.[3]

SOLUTION FOR NORMAL CARBONIC ANHYDRASE ACTIVITY (CATALYZED CASE) In this case it is assumed that the concentrations of H_2CO_3 and HCO_3^- depart only slightly from values that would be in equilibrium with CO_2, so that

$$C_{2c} \simeq \frac{K_4 C_{1c}}{C_{4c}} = \frac{K_1 K_2 C_{1c}}{C_{4c}} \tag{13}$$

$$C_{3c} \simeq K_1 C_{1c}, \tag{14}$$

where $K_1 = k_1/k_{-1}$ and $K_2 = k_2/k_{-2}$ are equilibrium constants. Since it is assumed that pH is constant (C_{4c} = constant), Eqs. 13 and 14 can be substituted into Eq. 10 to give, upon rearrangement

$$C_{1c} = \frac{T_1}{T_3}\ln \xi + \frac{T_2}{T_3} \tag{15}$$

$$T_3 = D_{1c} + \frac{D_{2c}K_4}{C_{4c}} + D_{3c}K_1. \tag{16}$$

The constants T_1 and T_2 depend on the unknown solute concentrations at $\xi = 1$ and $\xi = r_2/r_1$, and must satisfy the condition

$$N_{1c} + N_{2c} + N_{3c} = N_{1m} + N_{2m} + N_{3m} \tag{17}$$

[3] k_1 has been reported to be $\sim 0.15\ s^{-1}$ (23), and k_2 and k_4 are estimated to exceed k_1 by factors of 10^8 (24) and 10^4 (17), respectively. Analyses by Smith et al. (19) and Goddard et al. (25) of reaction-diffusion problems analogous to ours, using the technique of singular perturbation and matched asymptotic expansions, indicate that reactions 2 and 4 are sufficiently rapid to justify the assumption of local equilibrium.

at both $\xi = 1$ and $\xi = r_2/r_1$, where N_{im} is the membrane flux of species i (see Eqs. 26 and 27 below), and N_{ic}, the intracellular flux, is evaluated using Eq. 1. In principle, each of the individual solute fluxes should be continuous at the intracellular membrane surfaces ($N_{ic} = N_{im}$), but replacement of two of the three differential equations by the algebraic Eqs. 13 and 14 affords the possibility of satisfying only two boundary conditions. Continuity of tCO_2 flux was chosen to provide these conditions, as given in Eq. 17.

SOLUTION FOR TOTAL INHIBITION OF CARBONIC ANHYDRASE (UNCATALYZED CASE) In this case reaction 4 is eliminated and CO_2 and H_2CO_3 may no longer be assumed to be close to equilibrium, although this continues to be true for HCO_3^- and H_2CO_3, which are related according to

$$C_{3c} \simeq \frac{C_{2c}C_{4c}}{K_2}. \tag{18}$$

Eq. 18 substituted into Eq. 10 now provides an expression for the intracellular HCO_3^- concentration in terms of that of CO_2:

$$C_{2c} = (-C_{1c}D_{1c} + T_1 \ln \xi + T_2)/T_4 \tag{19}$$

$$T_4 = D_{2c} + \frac{D_{3c}C_{4c}}{K_2}. \tag{20}$$

Eqs. 18 and 19 may now be used to eliminate C_{2c} and C_{3c} from Eq. 4. The resulting solution for C_{1c} is

$$C_{1c} = a_I I_0(m\xi) + a_K K_0(m\xi) + \frac{T_5}{m^2}(T_1 \ln \xi + T_2) \tag{21}$$

$$m^2 = \frac{r_1^2}{D_{1c}}\left(k_1 + \frac{k_{-1}\, C_{4c}D_{1c}}{T_4K_2}\right) \tag{22}$$

$$T_5 = \frac{r_1^2 k_{-1} C_{4c}}{D_{1c}T_4K_2}, \tag{23}$$

where $I_0(x)$ and $K_0(x)$ are modified Bessel functions of the first and second kinds, respectively, of order zero. The constants to be determined are a_I, a_K, T_1, and T_2, and the boundary conditions to be satisfied are

$$N_{1c} = N_{1m} \tag{24}$$

$$N_{2c} + N_{3c} = N_{2m} + N_{3m} \tag{25}$$

at both $\xi = 1$ and $\xi = r_2/r_1$. A comparison of the solutions for "fast" and "slow" intracellular reaction kinetics, Eqs. 15 and 21, respectively, indicates that the Bessel function terms in the latter account for the finite reaction rate constants, the solutions otherwise being of the same form.

Membrane Fluxes

Very little information is available concerning the transport of the CO_2-containing species across the individual cell membranes of the epithelium. Transport of each will be assumed to

be passive and not coupled to that of other substances (including water), and the following simple expressions will be used:

$$N_{im} = P_i[C_i(-) - C_i(+)], \text{ i} = 1 \text{ or } 3 \tag{26}$$

$$N_{2m} = P_2\Delta\psi \frac{C_2(-) - C_2(+)\, e^{-\Delta\psi}}{1 - e^{-\Delta\psi}}, \tag{27}$$

where P_i is the permeability coefficient of solute i and $C_i(-)$ and $C_i(+)$ are solute concentrations at the sides of the membrane corresponding to smaller r and greater r, respectively. At $r = r_1$, $C_i(-) = C_i(r_1)$ and $C_i(+) = C_{ic}(r_1)$, whereas at $r = r_2$, $C_i(-) = C_{ic}(r_2)$ and $C_i(+) = C_{ib}$. Eq. 27 is derived using the constant field approximation (26), and $\Delta\psi = \psi(+) - \psi(-)$ is an electrical potential difference (dimensionless). ψ is the electrical potential divided by RT/F, the product of the gas constant and temperature divided by Faraday's constant ($RT/F = 26.7$ mV at 37°C).

The stoichiometry of the interconversion of CO_2 and HCO_3^- indicates that equal amounts of H^+ and HCO_3^- are formed or consumed by the intracellular reactions. It will be assumed that the net efflux of H^+ from the cell equals that of HCO_3^-, and that there is net H^+ transport across the luminal (brush border) cell membrane only. Accordingly, the H^+ flux is related to those of HCO_3^- by

$$N_{4m|r_1} = N_{2m|r_1} - (r_2/r_1)\, N_{2m|r_2}. \tag{28}$$

Thus, an expression relating the kinetics of H^+ secretion to the intracellular pH, luminal pH, and other variables is not required by this formulation.

Transport in the Tubule Lumen

In the proximal tubule, where the pH does not decline below ~6 (1), changes in the concentration of H^+ are insignificant compared with the flux of H^+ across the cell membrane. Thus, all of the H^+ secreted may be considered to be consumed in titrating luminal buffers, and conservation equations once again are required only for CO_2, HCO_3^-, and H_2CO_3. Assuming a steady state and symmetry about the z-axis, and neglecting axial diffusion and entrance effects,[4] these equations become (21)

$$\frac{\partial}{\partial z}(v_z C_i) = -\frac{1}{r}\frac{\partial}{\partial r}(rN_i) + S_i, \tag{29}$$

where v_z is the axial component of the fluid veolcity and N_i is the radial component of the solute flux, as in Eq. 1. According to the assumptions discussed above, reaction 1 is the only

[4]Our analysis (Eq. 35 especially) is not valid in the region near $z = 0$, where the concentration profiles change very rapidly with increasing z. The length (z_e) of this "entrance region" may be estimated by analogy with the well-known result for heat transfer from a fluid to a tube with walls maintained at constant temperature (27): $z_e/r_1 \simeq 0.2(v_0 r_1/D_0)$ where v_0 is the mean axial velocity at $z = 0$, and D_0 is a characteristic diffusivity. Taking the values for v_0 and r_1 in Table I, and choosing $D_0 = 10^{-5}\text{cm}^2\text{s}^{-1}$, $v_0 r_1/D_0 \simeq 5$ and $z_e \simeq r_1$. Since all results to be reported are for $z \geq 25r_1$, the entrance region should have a negligible effect. With regard to axial diffusion, the results in Figs. 3 and 6 can be used to confirm that almost all transport in the z-direction is by convection. The maximum contribution of axial diffusion is ~0.5%.

homogeneous reaction to be considered, and the reaction rates are given by

$$S_1 = k_{-1} C_3 - k_1 C_1 \tag{30}$$

$$S_2 = 0 \tag{31}$$

$$S_3 = -S_1. \tag{32}$$

Assuming that the rate of fluid reabsorption is independent of z, and noting that the Reynolds number in the proximal tubule is sufficiently small ($\sim 10^{-2}$) that inertial effects are absent, a simple analytical expression may be used for v_z (28):

$$v_z = 2(v_0 - 2v_{r1}\eta)(1 - \xi^2) \tag{33}$$

where v_0 is the mean velocity at $z = 0$ and η is a dimensionless axial coordinate: $\eta = z/r_1$. The dimensionless radial coordinate ξ is as defined previously.

To minimize numerical computations, approximate solutions for the luminal concentration profiles are sought which satisfy an integral form of Eq. 29:

$$\frac{\mathrm{d}}{\mathrm{d}\eta}\int_0^1 v_z C_i \, \xi \mathrm{d}\xi = -N_{i|\xi=1} + r_1 \int_0^1 S_i \xi \mathrm{d}\xi. \tag{34}$$

The concentration profiles are assumed to be of the form

$$C_i(\eta, \xi) = b_{1i}(\eta) + b_{2i}(\eta)\, \xi^2, \tag{35}$$

which satisfies the condition $\partial C_i/\partial \xi = 0$ at $\xi = 0$. The functions $b_{1i}(\eta)$ and $b_{2i}(\eta)$ are to be determined for CO_2, HCO_3^-, and H_2CO_3, and must satisfy the boundary conditions at $\xi = 1$. These involve the rates of the heterogeneous reactions:

$$N_i + \phi_i = N_{im} \text{ at } \xi = 1, \tag{36}$$

where ϕ_i is the total rate of creation of species i per unit surface area by reaction. Reactions 2 and 4 are those assumed to be occurring at this surface, so that

$$\phi_1 = \phi_1^{(4)} = k_{-4s} C_2 C_4 - k_{4s} C_1 \tag{37}$$

$$\phi_2 = \phi_2^{(2)} + \phi_2^{(4)} = \phi_2^{(2)} - \phi_1 \tag{38}$$

$$\phi_3 = \phi_3^{(2)} = -\phi_2^{(2)}, \tag{39}$$

where the superscripts refer to reactions 2 or 4, and k_{4s} and k_{-4s} are the forward and reverse rate constants for reaction 4, per unit surface area. During complete inhibition of carbonic anhydrase, it is assumed that $\phi_1 = 0$.

Throughout the tubule lumen, the H^+ concentration (C_4) is evaluated using the H_2CO_3/HCO_3^- equilibrium (Eq. 18). The assumption that all of the secreted H^+ is consumed in titrating luminal buffers (bicarbonate) leads to an expression for $\phi_2^{(2)}$

$$\phi_2^{(2)} = N_{4m|\xi=1} + \phi_1. \tag{40}$$

Accordingly, kinetic data are not required for reaction 2.

The functions $b_{1i}(\eta)$ and $b_{2i}(\eta)$ are also directly related to the "bulk" or "mixed mean" concentrations in the lumen, which are defined as

$$\bar{C}_i(\eta) \equiv \frac{\int_0^1 C_1 v_z \xi d\xi}{\int_0^1 v_z \xi d\xi} = b_{1i} + \frac{b_{2i}}{3}. \tag{41}$$

If the bulk concentrations are specified for a given value of η, all of the unknowns appearing in the expressions for the luminal and intracellular concentration profiles may be evaluated. The six membrane fluxes N_{im} (for i = 1,2,3 at $\xi = 1$ and $\xi = r_2/r_1$) are first eliminated by using Eqs. 26 and 27 in Eqs. 17, 24, and 25. There remain 17 unknowns common to both the catalyzed and uncatalyzed cases: b_{1i}, b_{2i}, C_{ic} ($\xi=1$), C_{ic} ($\xi=r_2/r_1$), T_1, T_2, N_{4m} ($\xi=1$), ϕ_1, and $\phi_2^{(2)}$, where i = 1, 2, 3. The additional constants a_I and a_K appear in the uncatalyzed case, for a total of 19. These unknowns are determined by numerical solution of appropriate sets of linear equations. The 11 equations common to both cases are provided by Eqs. 11, 12, 28, 36 (i = 1, 2, 3), 37, 40, and 41 (i = 1, 2, 3). The additional six equations needed for the catalyzed case are Eqs. 13, 14, and 17 (each applied twice, at $\xi = 1$ and $\xi = r_2/r_1$); the additional eight equations for the uncatalyzed case are Eqs. 18, 19, 24, and 25 (each at $\xi = 1$ and $\xi = r_2/r_1$).

The composition of the glomerular filtrate or tubule perfusate provides initial values of the bulk concentrations, $\bar{C}_i(0)$, and the only problem remaining is to determine the variation in bulk concentration with axial position, η. Evaluating the integral on the left-hand side of Eq. 34 using the definition of bulk concentration (Eq. 41), we obtain

$$\frac{1}{2}\frac{d}{d\eta}[\bar{C}_i(v_0 - 2v_{rl}\eta)] = -N_{il\xi=1} + r_1 \int_0^1 S_i \xi d\xi. \tag{42}$$

The right-hand side of this equation is readily evaluated using Eqs. 1, 30–32, and 35. The result is three coupled differential equations, which may be integrated numerically to determine $\bar{C}_i(\eta)$. At each step of the integration it is necessary to solve the system of linear equations discussed above to determine the right-hand side of Eq. 42.

A quantity of considerable interest experimentally is the amount of tCO_2 reabsorbed per unit length of tubule, termed J_{tCO_2}. This is given in terms of bulk concentrations as

$$J_{tCO_2} = \frac{\pi r_1}{\eta}\{v_0 \Sigma[\bar{C}_i(0) - \bar{C}_i(\eta)] + 2v_{rl}\eta\Sigma\bar{C}_i(\eta)\}, \tag{43}$$

where the length of tubule under consideration is $L = \eta r_1$, and the summations include, as usual, CO_2, HCO_3^-, and H_2CO_3.

RESULTS

Model Parameters

Values of the model parameters employed in most of the simulations are shown in Table I. The diffusivities for the various species in tubule fluid and cell cytoplasm were assumed comparable to those reported by Gros and Moll (29) for water and concentrated protein solutions, respectively, at 22°C. Diffusivities at 37°C are expected to be 30–40% larger, but adjusting these values has little effect on calculated reabsorption rates for tCO_2. In both compartments the diffusivity of H_2CO_3 was assumed equal to that of HCO_3^-, since the molecular weights are nearly identical. Permeabilities for CO_2 were estimated from values

measured by Roughton for red blood cell membranes (30). It has not been possible to measure H_2CO_3 permeability in the presence of CO_2; we assume it is similar to the value reported by Gutknecht et al. (31) for acetic acid in lipid bilayer membranes. To account for the increase in surface area due to the brush border microvilli and basal infoldings, the measured permeabilities were increased at r_1 and r_2 by factors of 36 and 20, respectively, based on the surface areas reported by Welling and Welling (14). The HCO_3^- permeability at r_1 is equal to that reported by Warnock and Burg (32) for the permeability of the entire epithelial layer in rabbit proximal straight tubule, our assumption being that the luminal membrane is the limiting resistance. The value shown is about a factor of two larger than that obtained by applying the area correcting factor to the value obtained by Gutknecht et al. (31) for lipid bilayers. The HCO_3^- permeability at r_2 is derived by fitting the computed reabsorption rate of tCO_2 to that reported by Lucci et al. (33), as discussed below.

The equilibrium constants K_1 and K_4 and the rate constant k_1 were obtained from the literature (15,23), and K_2 was calculated from $K_2 = K_4/K_1$. No information is available on the kinetics of the postulated heterogeneous reaction catalyzed by carbonic anhydrase at the luminal membrane surface. The value of the rate constant k_{4s} was chosen arbitrarily so that >99% of the secreted H^+ was consumed by this reaction; larger values would have no effect on our results. During total inhibition of carbonic anhydrase, we assume that $k_{4s} = 0$. As already discussed, values of the rate constants k_2 and k_4 are not required in the computations.

Plasma concentrations (C_{ib}) in Table I correspond to an assumed partial pressure of CO_2 (P_{CO_2}) of 40 mm Hg and pH of 7.4, representative of systemic blood. Recent findings of DuBose et al. (10) indicate that intrarenal P_{CO_2} may be significantly higher than this, some 60 mm Hg, and some of the simulations were performed using this value (see below). Intracellular pH appears to be quite uncertain; $pH_c = 7.0$ is representative of measurements in a variety of other cell types (34) and was chosen as a reference value.

The tubule radii shown in Table I are representative of those in the rat (13). The fluid velocities (v_0 and v_{r1}) are calculated from the study of Lucci et al. (33) involving in vivo perfusion of rat proximal tubules, since these data were used in estimating $P_2(r_2)$. The fraction of fluid reabsorbed by the transcellular pathway (f) was set arbitrarily at 0.5; the value of this parameter proves to be of little consequence, as will be discussed. Finally, the dimensionless transmembrane potential differences ($\Delta\psi_1$ and $\Delta\psi_2$) in Table I correspond to potentials of -3 mV in the lumen and -70 mV in the cell, relative to plasma (35).

Results for Normal Carbonic Anhydrase Activity

For the input values listed in Table I the computed reabsorption rate of tCO_2 is 150 pmol mm^{-1} min^{-1}, which is comparable to the experimental value of 147 ± 23 pmol mm^{-1} min^{-1} reported by Lucci et al. (33) for the rat. Fig. 3 shows concentration profiles for HCO_3^-, CO_2, H_2CO_3, and H^+ calculated under these conditions. Concentrations (or pH) are plotted as functions of the radial coordinate $\xi = r/r_1$ for several values of the axial coordinate $\eta = z/r_1$. In each instance radial variations in the solute concentrations are relatively small. For HCO_3^-, for example, the concentration declines only ~ 0.1 mM from the centerline ($\xi = 0$) to the membrane surface ($\xi = 1$). Nonetheless, the HCO_3^- concentration gradient is large enough that two-thirds of the HCO_3^- flux from the luminal fluid to the membrane surface at $\xi = 1$ is due to diffusion, with the remaining one-third being due to convection.

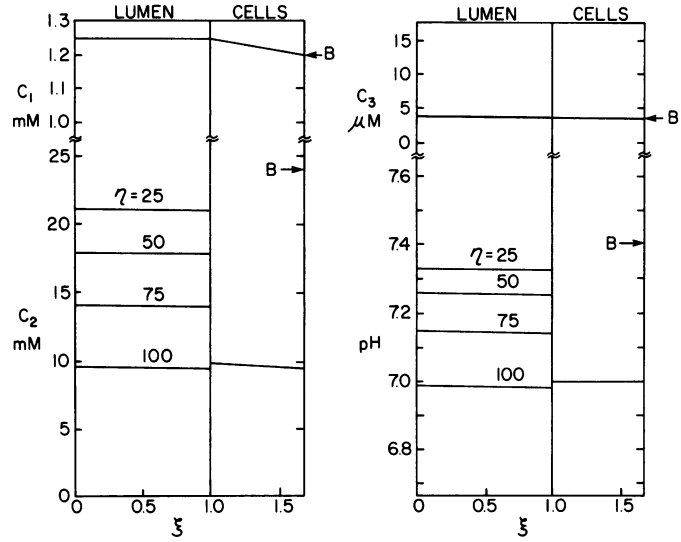

FIGURE 3 Radial and axial variations in CO_2, HCO_3^-, and H_2CO_3 concentrations (C_1, C_2, and C_3, respectively) and pH, calculated assuming normal carbonic anhydrase activity. Relative radial position is given by ξ, ξ=0 denoting the center of the lumen, and ξ=1, the brush border membrane. Axial position is indicated by η, also expressed relative to the tubule radius; curves where η is not specified indicate results that are independent of η. Assumed concentrations in peritubular plasma are denoted by *B*. Values of input parameters are given in Table I.

As shown in Fig. 3, the luminal HCO_3^- concentration decreases progressively with increasing η. Luminal pH declines in parallel fashion, reaching a value of 7.0 at η = 100. Concentrations of CO_2 and H_2CO_3, however, are essentially independent of η (beyond the entrance region, $0 < \eta < \sim 1$). For the largest values of the axial coordinate shown, η = 100 (corresponding to a perfused length of 1.5 mm), 23% of the initial perfusate volume has been reabsorbed, indicating that the amounts of CO_2 and H_2CO_3 in the lumen, as well as that of HCO_3^-, decrease progressively with increasing η. J_{tCO_2} is also virtually independent of η, the values calculated for η = 30 and η = 100 differing by < 1%. In light of this, most results for J_{tCO_2} will be reported as averages up to η = 30.

Factors Contributing to Bicarbonate Reabsorption

A useful starting point for the analysis of the results just presented is the special case where $J_{tCO_2} = 0$. In this case the net reaction rates and membrane fluxes are all zero. For simplicity, suppose that the transepithelial potential difference and fluid reabsorption rates are both set to zero ($\Delta\psi_2 = -\Delta\psi_1 = 2.62$, and $v_{rl} = 0$). For the plasma concentrations shown in Table I, inspection of Eqs. 26 and 27 indicates that for all membrane fluxes to be zero, intracellular concentrations of CO_2, HCO_3^-, and H_2CO_3 must equal 1.20 mM, 1.76 mM, and 3.54×10^{-3} mM, respectively. These CO_2 and H_2CO_3 concentrations are equal to those in plasma, while the equilibrium HCO_3^- concentration is much less than that in plasma (1.76 vs. 24 mM) because of the negative intracellular potential. Under these conditions, an intracellular pH of 6.27 is required for there to be no net reaction. We denote this value as pH_0.

If the cells are now maintained at a pH more alkaline than pH_0 (i.e., by active H^+ secretion), the net intracellular reaction is the hydration of CO_2 to generate HCO_3^- and H^+, which in turn elevates the intracellular HCO_3^- concentration above the equilibrium value (1.76 mM). This will cause bicarbonate to diffuse out of the cell into the lumen at r_1 and into the peritubular fluid at r_2. The extent to which diffusion across the peritubular membrane is preferred to backleak into the lumen, the more efficient will be the overall process of bicarbonate reabsorption. Our calculations for normal carbonic anhydrase activity indicate that for an H^+ secretory flux of 3.07×10^{-9} mol cm^{-2} s^{-1}, tCO_2 reabsorption is only 2.65×10^{-9} mol cm^{-2} s^{-1}. At the luminal or brush border membrane, net reabsorption of total CO_2 reflects the difference between the membrane flux of CO_2 (3.12×10^{-9} mol cm^{-2} s^{-1}) and backleak of HCO_3^-. With the value selected for the rate constant k_{4s}, essentially all of the secreted H^+ titrates HCO_3^- to form CO_2 by the catalyzed reaction; there is little formation of H_2CO_3 at this surface by the uncatalyzed reaction, and the membrane flux of H_2CO_3 is negligible.

The principal requirements for this reabsorptive process are the relatively alkaline intracellular pH ($pH_c > pH_0$) and the preferential secretion of H^+ into the lumen. The rate of fluid reabsorption, the transepithelial potential difference, and the solute permeabilities of the two membranes (especially to HCO_3^-) are also expected to influence its efficiency. The effects of these individual factors will be examined now in more detail.

Effects of Intracellular pH

The influence of intracellular pH on J_{tCO_2} is illustrated in Fig. 4. The solid curve labeled "P_{CO_2} = 40 mm Hg" gives results for the input concentrations and other parameters in Table I, and as expected from the discussion above, J_{tCO_2} is almost zero at $pH_c = 6.3$. The great sensitivity of J_{tCO_2} to pH_c is apparent, J_{tCO_2} increasing by a factor of 4 as pH_c is increased from 7.00 to 7.54. The solid curve labeled "P_{CO_2} = 60 mm Hg" corresponds to P_{CO_2} values representative of those reported recently by DuBose et al.(10).[5] In this case the "zero net reaction pH" is somewhat lower ($pH_0 = 6.08$), causing the curve to be shifted to the left, but the results are qualitatively similar.

Effects of Convection and Transepithelial Potential Difference

Even in the absence of H^+ secretion, reabsorption of fluid will tend to concentrate the luminal contents, creating concentration gradients favoring reabsorption of tCO_2, primarily by diffusion of CO_2 (the most permeable species). The influence of convection on transport within the cell is negligible, however; for the normal parameter values in Table I, values of J_{tCO_2} calculated for $f = 0$ and $f = 1$ are within 0.02%. Thus, the pathway followed by reabsorbed water has little influence on J_{tCO_2}. If the transepithelial potential difference is eliminated ($\Delta\psi_2 = -\Delta\psi_1 = 2.62$), with all other parameter values normal, J_{tCO_2} is reduced ~ 7% below the control value of 150 pmol mm^{-1} min^{-1}.

---

[5]DuBose et al. (10) did not report values of intrarenal HCO_3^- concentration and pH corresponding to their measured values of P_{CO_2}. We estimate these assuming that the values of C_{ib} in Table I are representative of arterial plasma and that tCO_2 concentrations in arterial and peritubular plasma are the same. We obtain C_{1b} = 1.81 mM, C_{2b} = 23.4 mM, and pH_b = 7.21 for an intrarenal P_{CO_2} of 60 mm Hg.

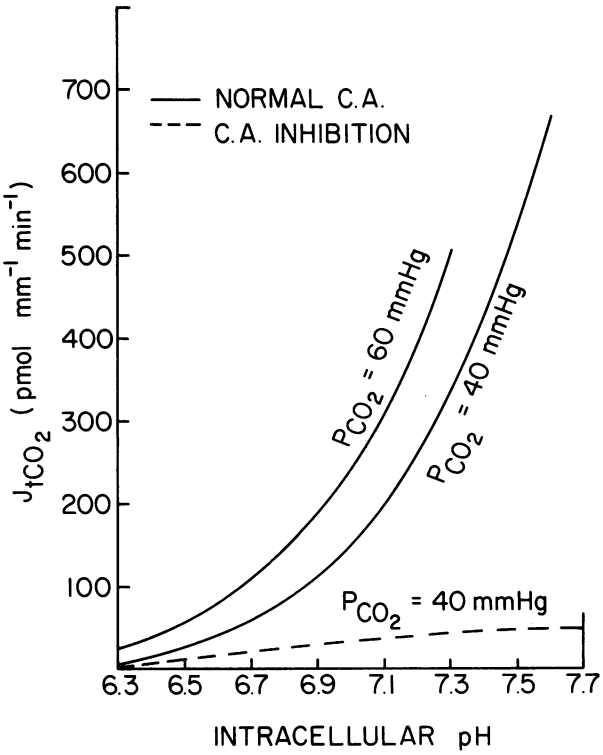

FIGURE 4 Effect of intracellular pH on reabsorption of tCO_2. Results are shown for two different assumed values of P_{CO_2} in peritubular blood, and for either normal activity of or complete inhibition of carbonic anhydrase (C.A.)

Effects of Membrane Permeabilities

Simulations in which both CO_2 permeabilities (at r_1 and r_2) are 1/10 or 10 times the values given in Table I give values of J_{tCO_2} differing from one another by $< 0.1\%$. This result is expected, since the permeabilities to CO_2 are high and the membranes therefore do not offer significant resistances to CO_2 diffusion. Under normal, catalyzed reaction conditions the values of the H_2CO_3 membrane permeabilities also do not affect J_{tCO_2}. This is because, as already mentioned, the catalyzed surface reaction prevents the accumulation of H_2CO_3 in the lumen.

The HCO_3^- permeability at r_1 also proves to be of little consequence. For a fixed value of the permeability at r_2, $P_2(r_1)$ values ranging from 0 to 2.0×10^{-5} cm/s altered J_{tCO_2} by $< 1\%$. Although the net intracellular reaction rate is increased for higher HCO_3^- permeabilities at r_1, the backleak of HCO_3^- into the lumen increases by a nearly identical amount. Thus, transport of HCO_3^- out of the cell at r_2 is almost unchanged and only the efficiency of the process is affected.

The critical membrane permeability for the catalyzed case is that for HCO_3^- at r_2. As shown in Fig. 5 there is a linear relationship between J_{tCO_2} and $P_2(r_2)$. The line does not pass through the origin because, although there is no transport of HCO_3^- from cell to blood when $P_2(r_2) = 0$, some diffusion of CO_2 takes place as a result of the concentration gradient

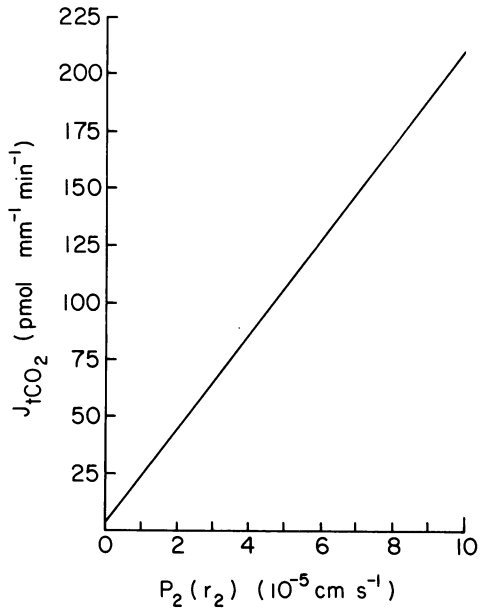

FIGURE 5 Effect of HCO_3^- permeability at the basal cell membrane on the reabsorption of tCO_2. Calculations assume normal carbonic anhydrase activity.

established by water reabsorption. For an assumed intracellular pH of 7.0, $P_2(r_2) = 7.0 \times 10^{-5}$ cm/s is required to give a value of J_{tCO_2} comparable to that measured by Lucci et al. (33), ~150 pmol mm^{-1} min^{-1}. Higher assumed values of pH_c would correspond to lower values of $P_2(r_2)$ and lower values of pH_c to higher values of $P_2(r_2)$, as indicated by the combined results of Figs. 4 and 5.

Effects of Complete Carbonic Anhydrase Inhibition

Total inhibition of carbonic anhydrase (as with infusion of sufficient dosages of acetazolamide or benzolamide) is assumed to eliminate reaction 4 both in the cell cytoplasm and at the luminal membrane surface. Acetazolamide infusion has also been found to reduce proximal fluid reabsorption to 30–50% of the control level in the rat (6,33). In our simulations v_{rl} is assumed to be reduced from 4.1×10^{-5} cm/s to 1.4×10^{-5} cm/s, based on the results of Lucci et al. (33). Under these conditions J_{tCO_2} was calculated to be 37.5 pmol mm^{-1} min^{-1}, or 25% of the normal value. Radial concentration profiles for carbonic anhydrase inhibition are illustrated in Fig. 6. As with the normal case, radial variations in CO_2 and HCO_3^- concentrations are quite small. The transepithelial difference in P_{CO_2} in the uncatalyzed case (0.6 mm Hg) is about one-third of that calculated for normal conditions (1.6 mm Hg). Also, as seen before, the bulk concentrations of CO_2 and H_2CO_3 are nearly independent of z. The principal difference is the buildup of H_2CO_3 near the luminal membrane surface (Fig. 6), resulting from the increased production of H_2CO_3 by the uncatalyzed titration of HCO_3^-. For the parameter values used (Table I), ~70% of the H_2CO_3 so formed is calculated to diffuse across the luminal membrane, the remainder diffusing into the lumen to be converted to CO_2. Accordingly, most of the tCO_2 transport across this membrane is in the form of H_2CO_3

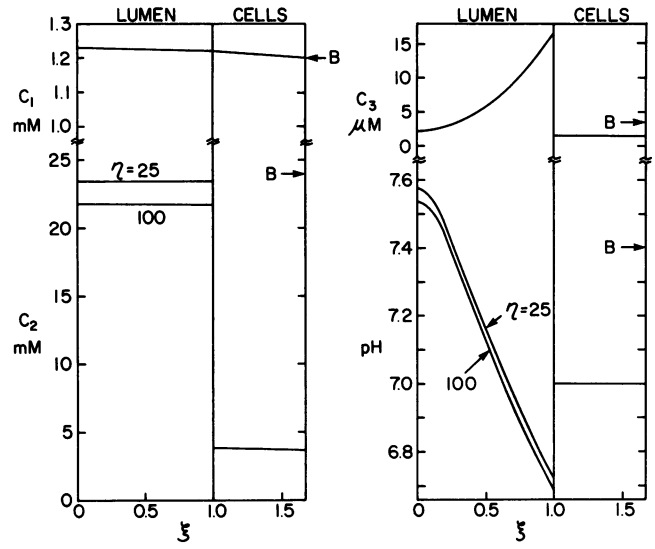

FIGURE 6 Radial and axial variations in CO_2, HCO_3^-, and H_2CO_3 concentrations and pH, calculated assuming complete inhibition of carbonic anhydrase. For definitions of symbols, see Fig. 3.

(0.538×10^{-9} mol cm^{-2} s^{-1}), with a smaller contribution from CO_2 (0.236×10^{-9} mol cm^{-2} s^{-1}), and the net transport again being diminished by a backleak of HCO_3^- (0.110×10^{-9} mol cm^{-2} s^{-1}).

Based on this information, it is expected that J_{tCO_2} in the uncatalyzed case will be sensitive to the H_2CO_3 permeability of the brush border membrane, $P_3(r_1)$, although this is not true under normal circumstances. This linear relationship is illustrated in Fig. 7. As shown by the dashed curve in Fig. 4, carbonic anhydrase inhibition is also calculated to reduce the sensitivity of J_{tCO_2} to variations in intracellular pH. At any given value of pH_c, J_{tCO_2} is lower for the uncatalyzed than for the catalyzed case, as expected.

Effects of Intracellular Reaction Rate

Partial inhibition of intracellular carbonic anhydrase may be simulated by using the same basic formulation as for total inhibition, but not setting $k_4 = k_{-4} = 0$ (as was done in deriving Eqs. 21–23). The only changes required are in the definitions of the constants m^2 and T_5:

$$m^2 = \frac{r_1^2}{D_{1c}}\left[k_1 + k_4 + \frac{C_{4c}D_{1c}}{T_4}\left(k_{-4} + \frac{k_{-1}}{K_2}\right)\right] \tag{44}$$

$$T_5 = \frac{C_{4c}r_1^2}{T_{4c}D_{1c}}\left(k_{-4} + \frac{k_{-1}}{K_2}\right). \tag{45}$$

Since the ratio k_4/k_{-4} is fixed by equilibrium, this change requires knowledge of one additional reaction rate constant (e.g., k_4).

Fig. 8 shows a plot of J_{tCO_2} as a function of $k_t = k_1 + k_4$, with all other inputs as given in Table I. The relationship is clearly very nonlinear. For complete inhibition $k_t = k_1 = 0.15$ s^{-1} (uncatalyzed rate), and it can be seen that increases in k_t up to ~ 100 times this value produce

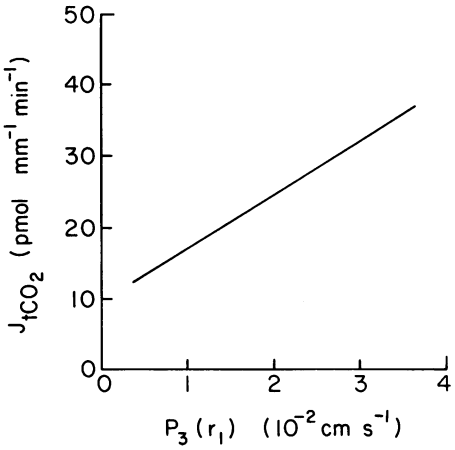

FIGURE 7

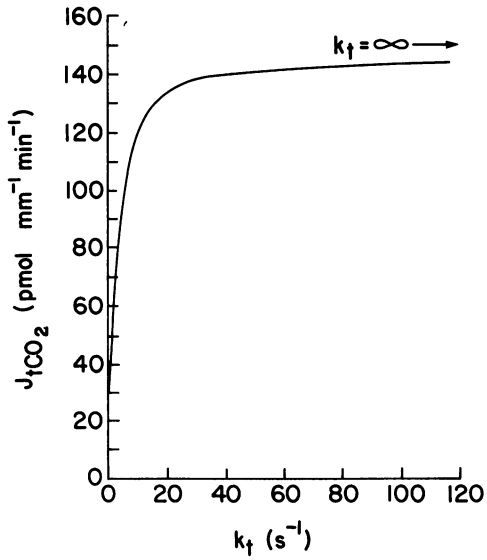

FIGURE 8

FIGURE 7 Effect of H_2CO_3 permeability at the brush border membrane on the reabsorption of tCO_2. Calculations assume total inhibition of carbonic anhydrase.

FIGURE 8 Effect of overall intracellular reaction rate constant ($k_t = k_1 + k_4$) on reabsorption of tCO_2. All other parameters, including the rate constant for CO_2 hydration at the brush border membrane, have the normal values given in Table I.

large increases in J_{tCO_2}, but further increases have relatively little effect. In the absence of inhibitors k_4 is estimated to be larger than k_1 by a factor of 10^4 (17), so that k_t normally will be of the order of 10^3 s^{-1}. For large values of k_t, J_{tCO_2} can be seen in Fig. 8 to approach a value equivalent to that obtained using the formulation for infinitely fast reaction (indicated as $k_t = \infty$), as expected. The results in Fig. 8 show that even if k_4 is reduced to ~1% of its normal value, J_{tCO_2} will still be 80–90% of normal. For k_t to closely approach the uncatalyzed value ($k_4 \ll k_1$), k_4 would have to be reduced by a factor of at least 10^5, corresponding to ~99.999% inhibition. This may explain in part the inconsistent degree to which J_{tCO_2} has been found to be reduced in the presence of carbonic anhydrase inhibitors (6–8,33,36).

DISCUSSION

A principal motivation for this study was to provide additional insight in areas where experimental results have been absent or contradictory, particularly with regard to the role of carbonic anhydrase and the magnitude of the transepithelial difference in P_{CO_2}. In the presence of apparently maximal inhibitory dosages of acetazolamide or benzolamide, bicarbonate or tCO_2 reabsorption has been reported to range from ~50% of normal (7,8) to not more than ~15% of normal (33,36). A recent free-flow micropuncture study in the rat by Cogan et al. (6), which appears to be free of many of the technical limitations of earlier studies in the rat, reports tCO_2 reabsorption during acetazolamide infusion to be 20% of normal. We calculated a very similar value in simulations of complete inhibition, J_{tCO_2} being 25% of normal. Although this agreement may be fortuitous, since there is considerable

uncertainty in the estimate of H_2CO_3 membrane permeability, it indicates nonetheless that this experimental result is fully consistent with reaction rate constants and transport parameters available from the literature.[6] As already described, H_2CO_3 diffusion from lumen to cell is calculated to account for some 70% of net tCO_2 transport out of the tubule fluid during carbonic anhydrase inhibition, indicating that the carbonic acid recycling scheme proposed by Rector (1,37) is quite viable. It may be added that in the absence of significant H_2CO_3 transport, Cogan et al. (6) estimate that a relatively high intracellular pH ($pH_c > 8$) is required to give an intracellular reaction rate sufficiently large to explain their results.

It has long been assumed that the P_{CO_2} throughout the renal cortex is similar to that in arterial plasma, but several recent studies have challenged this. Karlmark and Danielson (11) have argued that the P_{CO_2} in proximal tubule fluid is significantly higher than in either arterial or peritubular plasma, and recent microelectrode measurements reported by Sohtell (9) indicate differences frequently exceeding 20 mm Hg. By contrast, using another microelectrode technique, DuBose et al. (10) were unable to detect differences in P_{CO_2} between proximal tubule lumen and peritubular (efferent arteriolar) blood, although P_{CO_2} at both sites was found to be ~25 mm Hg greater than in arterial plasma. Our calculated results for normal conditions are in agreement with the latter authors, in that the 1.6 mm Hg difference in P_{CO_2} that we find undoubtedly is too small to be detected using present experimental methods. This calculation is based on the reasonable assumption that the membrane resistances to CO_2 transport are negligible and that the diffusion coefficient for CO_2 in the cell is similar to that reported for concentrated protein solutions (29). Warnock and Rector (2) discuss other data that indicate that the cellular resistance to CO_2 diffusion is not unlike an equivalent layer of water, and that transepithelial differences in P_{CO_2} of more than a few millimeters Hg are unlikely. Our results do not allow any conclusions to be reached about the absolute level of plasma P_{CO_2} in the renal cortex. We arbitrarily adopted the "classical" value of 40 mm Hg (representative of arterial blood) for most of our calculations; similar results are obtained for elevated P_{CO_2} values (such as those of DuBose et al.) if the assumed intracellular pH is reduced slightly (Fig. 4).

A limitation of the present model is the neglect of nonbicarbonate buffers in the tubule lumen, such as ammonia and phosphate. Although of only secondary importance in early portions of the proximal tubule, where HCO_3^- concentration is still high, these substances will gain significance in later portions of the tubule and in certain experimental conditions. The metabolic production rate of CO_2 is probably relatively small and also was neglected, but could be readily included as a source term in Eq. 4. Possibly a more significant limitation is that variations in luminal pH in the model have no direct effect on the rate of H^+ secretion, whereas it has been suggested that H^+ secretion should obey pump-leak kinetics, reaching

---

[6]Values of k_1 and K_1 lower than those given in Table I have been reported recently (15), 0.08 s^{-1} and 2.50×10^{-3}, respectively. Based on this new value of K_1 and the value of K_4 given in Table I, K_2 is calculated to be 3.18×10^{-7} mol cm^{-3}. Using these constants J_{tCO_2} during complete inhibition of carbonic anhydrase is calculated to be 19% of normal, as compared with the experimental value of 20% (6) and the value of 25% calculated using the parameters in Table I. Increasing the diffusivities in Table I by a factor of 1.4 to give values more closely corresponding to those expected at 37°C reduces the calculated J_{tCO_2} by an additional small amount, to 17% of normal. These differences in k_1, K_1, K_2, and diffusivities have negligible effect on J_{tCO_2} during normal carbonic anhydrase activity, since carbonic acid transport in this case does not play a significant role.

zero at a luminal pH of ~6.4 (12). An additional variable(s) would have to be introduced to simulate this behavior (e.g., variable pH_c) and the numerical solution scheme modified accordingly. For these reasons, the present model is best applied to early portions of the proximal tubule, where neither HCO_3^- concentration nor pH have reached low levels.

We wish to thank Dr. D. G. Warnock for originally bringing this problem to our attention, and he and Doctors M. G. Cogan, D. A. Maddox, and F. C. Rector, Jr. for their continuing interest in this work. We also wish to acknowledge the expert secretarial assistance of Debora Hackel.

This work was supported by a grant from the National Institutes of Health (AM 20368).

Received for publication 29 September 1979 and in revised form 15 January 1980.

REFERENCES

1. RECTOR, F. C., Jr. 1976. Renal acidification and ammonia production; chemistry of weak acids and bases; buffer mechanisms. *In* The Kidney. B. M. Brenner and F. C. Rector, Jr., editors. W.B. Saunders Co., New York, 318.
2. WARNOCK, D. G., and F. C. RECTOR, Jr. 1979. Proton secretion by the kidney. *Annu. Rev. Physiol.* **41**:197.
3. GIEBISCH, G., and G. MALNIC. 1976. Studies on the mechanism of tubular acidification. *Physiologist.* **19**:511.
4. MAREN, T. H. 1974. Chemistry of the renal reabsorption of bicarbonate. *Can. J. Physiol. Pharmacol.* **52**:1041.
5. LEVINE, D. Z. 1978. Difficulties in the micropuncture evaluation of proximal renal bicarbonate reabsorption: an overview for the general reader. *Can. J. Physiol. Pharmacol.* **56**:354.
6. COGAN, M.G., D. A. MADDOX, D. G. WARNOCK, E. T. LIN, and F. C. RECTOR, Jr. 1979. The effect of acetazolamide on bicarbonate reabsorption in the proximal tubule of the rat. *Am. J. Physiol.* **237**:F447.
7. KUNAU, R. T., Jr. 1972. The influence of the carbonic anhydrase inhibitor benzolamide (C1-11, 366) on the reabsorption of chloride, sodium, and bicarbonate in the proximal tubule of the rat. *J. Clin. Invest.* **51**:294.
8. VIERA, F. L., and G. MALNIC. 1968. Hydrogen secretion by rat renal cortical tubules as studied by an antimony microelectrode. *Am. J. Physiol.* **214**:710.
9. SOHTELL, M. 1979. P_{CO_2} of the proximal tubular fluid and the efferent arteriolar blood in the rat kidney. *Acta Physiol. Scand.* **105**:137.
10. DUBOSE, T. D., Jr., L. R. PUCACCO, D. W. SELDIN, N. W. CARTER, and J. P. KOKKO. 1978. Direct determination of P_{CO_2} in the rat renal cortex. *J. Clin. Invest.* **62**:338.
11. KARLMARK, B., and B. G. DANIELSON. 1974. Titratable acid, pCO_2, bicarbonate and ammonia ions along the rat proximal tubule. *Acta Physiol. Scand.* **91**:243.
12. CASSOLA, A. C., G. GIEBISCH, and G. MALNIC. 1977. Mechanisms and components of renal tubular acidification. *J. Physiol. (Lond.).* **267**:601.
13. MAUNSBACH, A. B. 1973. Ultrastructure of the proximal tubule. *Handb. Physiol.* **8**:31.
14. WELLING, L. W., and D. J. WELLING. 1975. Surface areas of brush border and lateral cell walls in the rabbit proximal nephron. *Kidney Int.* **8**:343.
15. MAREN, T. H. 1978. Carbon dioxide equilibria in the kidney: the problems of elevated carbon dioxide tension, delayed dehydration, and disequilibrium pH. *Kidney Int.* **14**:395.
16. KERN, D. M. 1960. The hydration of carbon dioxide. *J. Chem. Educ.* **37**:14.
17. MAREN, T. H. 1967. Carbonic anhydrase: chemistry, physiology, and inhibition. *Physiol. Rev.* **47**:595.
18. KERNOHAN, J. C., W. W. FORREST, and F. J. W. ROUGHTON. 1963. The activity of concentrated solutions of carbonic anhydrase. *Biochim. Biophys. Acta.* **67**:31.
19. SMITH, K. A., J. H. MELDON, and C. K. COLTON. 1973. An analysis of carrier-facilitated transport. *AIChE J.* **19**:102.
20. GROS, G., W. MOLL, H. HOPPE, and H. GROS. 1976. Proton transport by phosphate diffusion. A mechanism of facilitated CO_2 transfer. *J. Gen. Physiol.* **67**:773.
21. BIRD, R. B., W. E. STEWART, and E. N. LIGHTFOOT. 1960. Transport Phenomena. John Wiley & Sons, Inc., New York, 559.
22. OLANDER, D. R. 1960. Simultaneous mass transfer and equilibrium chemical reaction. *AIChE J.* **6**:233.
23. MALNIC, G., and G. GIEBISCH. 1972. Mechanism of renal hydrogen ion secretion. *Kidney Int.* **1**:280.
24. GIBBONS, B. H., and J. T. EDSALL. 1963. Rate of hydration of carbon dioxide and dehydration of carbonic acid at 25°. *J. Biol. Chem.* **238**:3502.

25. GODDARD, J. D., J. S. SCHULTZ, and R. J. BASSETT. 1970. On membrane diffusion with near-equilibrium reaction. *Chem. Eng. Sci.* **25**:665.
26. GOLDMAN, D. E. 1943. Potential, impedance, and rectification in membranes. *J. Gen. Physiol.* **27**:37.
27. ECKERT, E. R. G., and R. M. DRAKE, Jr. 1972. Analysis of Heat and Mass Transfer. McGraw-Hill Book Company, New York, 337.
28. MACEY, R. I. 1963. Pressure flow patterns in a cylinder with reabsorbing walls. *Bull. Math. Biophys.* **25**:1.
29. GROS, G., and W. MOLL. 1974. Facilitated diffusion of CO_2 across albumin solutions. *J. Gen. Physiol.* **64**:356.
30. ROUGHTON, F. J. W. 1959. Diffusion and simultaneous chemical reaction velocity in haemoglobin solutions and red cell suspensions. *Prog. Biophys. Biophys. Chem.* **9**:55.
31. GUTNECKT, J., M. A. BISSON, and D. C. TOSTESON. 1977. Diffusion of carbon dioxide through lipid bilayer membranes. Effects of carbonic anhydrase, bicarbonate, and unstirred layers. *J. Gen. Physiol.* **69**:779.
32. WARNOCK, D. G., and M. B. BURG. 1977. Urinary acidification. CO_2 transport by the rabbit proximal straight tubule. *Am. J. Physiol.* **232**:F20.
33. LUCCI, M. S., D. G. WARNOCK, and F. C. RECTOR, Jr. 1979. Carbonic anhydrase-dependent bicarbonate reabsorption in the rat proximal tubule. *Am. J. Physiol.* **236**:F58.
34. WADDELL, W. J., and R. G. BATES. 1969. Intracellular pH. *Physiol. Rev.* **49**:285.
35. GIEBISCH, G, and E. E. WINDHAGER. 1973. Electrolyte transport across renal tubular membranes. *Handb. Physiol.* **8**:315.
36. BURG, M. B., and N. GREEN. 1977. Bicarbonate transport by isolated perfused rabbit proximal convoluted tubules. *Am. J. Physiol.* **233**:F307.
37. RECTOR, F. C., Jr. 1973. Acidification of the urine. *Handb. Physiol.* **8**:431.
38. COHEN, J. J., and D. E. KAMM. 1976. Renal metabolism: relation to renal function. *In* The Kidney. B.M. Brenner and F. C. Rector, Jr., editors. W. B. Saunders Co., New York. 126.